

# Manipulating Epileptiform Bursting in the Rat Hippocampus Using Chaos Control and Adaptive Techniques

Marc W. Slutzky, *Member, IEEE*, Predrag Cvitanovic, and David J. Mogul\*, *Member, IEEE*

**Abstract**—Epilepsy is a relatively common disease, afflicting 1%–2% of the population, yet many epileptic patients are not sufficiently helped by current pharmacological therapies. Recent reports have suggested that chaos control techniques may be useful for electrically manipulating epileptiform bursting behavior *in vitro* and could possibly lead to an alternative method for preventing seizures. We implemented chaos control of spontaneous bursting in the rat hippocampal slice using robust control techniques: stable manifold placement (SMP) and an adaptive tracking (AT) algorithm designed to overcome nonstationarity. We examined the effect of several factors, including control radius size and synaptic plasticity, on control efficacy. AT improved control efficacy over basic SMP control, but relatively frequent stimulation was still necessary and very tight control was only achieved for brief stretches. A novel technique was developed for validating period-1 orbit detection in noisy systems by forcing the system directly onto the period-1 orbit. This forcing analysis suggested that period-1 orbits were indeed present but that control would be difficult because of high noise levels and nonstationarity. Noise might actually be lower *in vivo*, where regulatory inputs to the hippocampus are still intact. Thus, it may still be feasible to use chaos control algorithms for preventing epileptic seizures.

**Index Terms**—Adaptive, control, epilepsy, chaos, hippocampus, periodic orbit, seizure, synaptic plasticity.

## I. INTRODUCTION

**M**ORE than 50 million people worldwide are afflicted with epilepsy, and over 20% of these people are not sufficiently helped by medications. The last resort for some of these patients is to have the seizure-generating part of the brain (the focus) surgically removed. While surgery is often successful in preventing seizures, it can have serious side effects such as memory loss or speech deficits. Therefore, many groups are working to develop less-invasive alternatives to surgery for treating drug-resistant epilepsy [1]. Two currently available therapies use electrical stimulation to stop seizures. These implants stimulate either the vagus nerve [2]–[5] or the centromedian thalamic nucleus [6]. They are moderately

successful at stopping seizures. Vagus nerve stimulators reduce the number of seizures by 50% or more in approximately 35%–40% of patients [7]. However, their mechanism of action is uncertain and they have several adverse effects [8]. In addition, direct stimulation of the brain at a set frequency could potentially kindle new epileptic foci in those areas. Finally, these stimulators have only been available for a few years, so their long-term sequelae are unknown. It has been suggested that chaos control techniques might be used to prevent or stop seizures with intermittent electrical stimuli [9]. These techniques possess the advantage of requiring relatively infrequent stimulation of the tissue. This would reduce the likelihood of inducing new epileptic seizures and decrease power requirements, both important considerations for an implanted device.

On an electroencephalogram (EEG), the period during which a seizure takes place is referred to as the ictal period; the period between seizures is, thus, the interictal period. One of the hallmarks of epilepsy is the presence of spikes in the EEG during this interictal period. While the precise role of interictal spikes in epileptogenesis is not currently certain [10]–[12], it is plausible that developing a method to control them could provide a way to control seizure activity as well. Bursts are the *in vitro* analogues of these spikes and can be induced to occur spontaneously in the transverse rat hippocampal slice providing an *in vitro* model of epilepsy. It has been suggested that spontaneous hippocampal bursting is chaotic and, therefore, chaos control techniques might be appropriate [9]. While this suggestion is somewhat controversial [13], previous studies have shown that unstable periodic orbits (UPOs) of low periods are highly prevalent in hippocampal bursting [14], and there have been reports of positive Lyapunov exponents suggesting that chaos exists in the EEG during seizures [15], [16].

A chaotic attractor can be described by a skeleton of UPOs [17]. These UPOs are periodic paths in state space to and from which the system recurrently approaches and recedes. The presence of UPOs in a system implies the presence of determinism and suggests chaos. Furthermore, the presence of UPOs strengthens the rationale for using chaos control techniques to manipulate bursting, since UPOs are the points around which control can be applied [9]. However, a relatively large component of randomness has also been detected in bursting [14] suggesting that chaos control might be difficult to achieve in practice, especially if the amplitude of the noise were larger than the region in which control was desired.

Manuscript received June 13, 2001; revised June 3, 2002. This work was supported in part by the National Institutes of Health (NIH) under Grant NS31764 and Grant 0830350K614 and in part by the Whitaker Foundation. *Asterisk indicates corresponding author.*

M. W. Slutzky is with the Department of Biomedical Engineering Northwestern University, Evanston, IL 60208 USA

P. Cvitanovic is with the Center for Nonlinear Science, Georgia Institute of Technology, Atlanta, GA 30332 USA.

\*D. J. Mogul is with the Department of Biomedical Engineering, Pritzker Institute of Biomedical Science and Engineering, Illinois Institute of Technology, 10 West 32nd Street, Chicago, IL 60616-3793 USA (e-mail: mogul@iit.edu).

Digital Object Identifier 10.1109/TBME.2003.810701

The goal of chaos control is to keep the system state point within a certain distance (the control radius  $R_c$ ) of the fixed point by capitalizing on the sensitivity of chaotic systems to small perturbations and thereby minimizing the amount of perturbations. Since the concept of controlling a chaotic system without *a priori* knowledge of the underlying dynamics was developed in 1990 by Ott *et al.* (OGY control, [18]), many chaos control algorithms have been advanced [19]–[22]. A simpler algorithm based on linear negative feedback control of a system parameter was used to control chaos in a diode resonator circuit [19]. A variant of OGY called proportional perturbation feedback (PPF) [21] modifies the system state point [viz., the interburst interval (IBI)] instead of a system parameter. We used a modification of PPF called stable manifold placement (SMP) [23] which is simpler and more robust than PPF because it requires less assumptions to be made about system parameters.

In this paper, we explore in detail the modification of bursting behavior using techniques from chaos control. Accurate fixed-point estimation is crucial to the success of chaos control. Therefore, in addition to SMP control, we implement for the first time in a biological system a method of continuously refining the fixed point and stable manifold estimates [24]. We also develop a novel protocol, *state-point forcing*, that helps determine the validity of fixed-point estimates and assesses the feasibility of chaos control.

## II. METHODS

### A. Experimental Methods

Male Sprague–Dawley rats, age 20–25 days, were anesthetized (Isoflurane) and decapitated. Cerebral hemispheres were removed, hemisected, and the hippocampus dissected out during perfusion with chilled artificial cerebrospinal fluid (ACSF) containing (in mM):  $\text{NaH}_2\text{PO}_4$  1.25,  $\text{MgSO}_4$  1.3, NaCl 124,  $\text{NaHCO}_3$  24, D-Glucose 10, KCl 3.5,  $\text{CaCl}_2$  2.4. Slices 400  $\mu\text{m}$  thick were cut using a tissue chopper (Stoelting; Wood Dale, IL). Slices were maintained in ACSF at room temperature, perfused by 95%  $\text{O}_2$ /5%  $\text{CO}_2$ . Slices were placed in the bottom of a 1-ml experimental bath under a dissecting microscope and perfused by oxygenated ACSF. The bath temperature was kept at  $35 \pm 1^\circ\text{C}$ , at a flow rate of 5–6 ml/min. Slices were allowed to equilibrate to the bath temperature for at least 20 min before initiating recording procedures. A glass micropipette recording electrode (3–5  $\text{M}\Omega$ ) was filled with 2 M NaCl and placed in the cell body layer of the CA3 region [Fig. 1(A)]. Bursting was induced by bathing the slices in ACSF containing high potassium concentration ( $[\text{K}^+]_o = 10.5 \text{ mM}$ ). A bipolar tungsten stimulating electrode was placed in the Schaffer collaterals. Stimuli consisted of single, 80  $\mu\text{s}$  square-wave current pulses with amplitudes 0.1–0.3 mA.

### B. Burst Detection

All equipment was electrically insulated from noise and vibrations using a Faraday cage and air table, respectively. Signals from the recording electrode were passed through a bandpass filter on an AC differential amplifier (DAM 80, World Precision

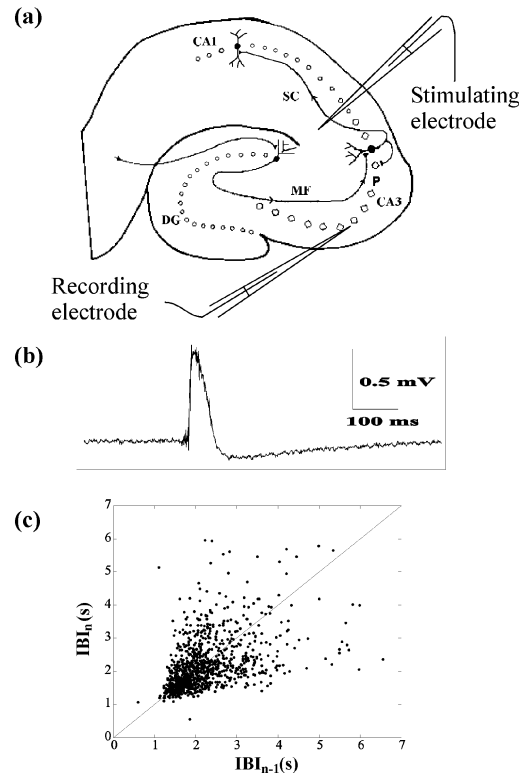


Fig. 1. Bursting in the hippocampal slice. (A) Schematic diagram of hippocampal slice organization. Granule cells in the dentate gyrus (DG) send mossy fiber (MF) axons to the CA3 region, where they synapse onto pyramidal cells. The recording electrode was placed in the pyramidal cell body layer (P) of the CA3 region. These cells send axons [Schaffer collaterals (SCs)] to the CA1 region. The stimulating electrode was placed among these axons. (B) An example of a spontaneous burst recorded extracellularly in the CA3 pyramidal layer. (C) A return map of 1000 IBIs recorded during spontaneous bursting. Fixed points lie along the identity ( $45^\circ$ ) line.

Instruments) with cutoff frequencies of 0.3 Hz and 3 kHz. Bursts were detected using an analog circuit consisting of a 20 dB/dec low-pass filter with unity gain and an adjustable window discriminator. The window discriminator [25] used a comparator to produce a two-state output: high (+5 V) if the input was between a low ( $V_L$ ) and high ( $V_H$ ) threshold and low (0 V) if the input was outside of this window. Since the recording amplifier had a gain of 1000, and burst amplitudes typically were on the order of 1 mV, the inputs to the window discriminator were on the order of 1 V. The low threshold  $V_L$  was set in the range of 60–400 mV, with potentiometers used to allow fine adjustment of the threshold. Settings for the low threshold varied because of the variation in noise amplitude in different experiments. However,  $V_L$  was constant within each experiment. The high threshold was set to at least 3 V. An additional criterion was added in the software to ensure that the positive detection was indeed a burst: the IBI had to be at least 250 ms.

A real-time data acquisition board (Adwin 4L, Keithley Instruments), which contained its own 486 microprocessor, recorded the IBIs, calculated when a stimulus needed to be delivered, and sent out the stimulus signal. The board's processor was programmed using a compiled version of BASIC called Adbasic. The host computer ran the neurocontrol software (written in Visual C++ 5.0) that performed fixed-point detection, adaptive control techniques, data storage, and display, and

enabled changes to system parameters and control techniques in real-time.

### C. UPO Detection

Each series of IBIs was delay embedded into two-dimensional (2-D) state space. The system state was, thus, visualized by plotting the current IBI versus the previous IBI—i.e., a return map. A recently developed transform technique [26] was used to search for unstable period-1 orbits (also known as fixed points) in real-time. This technique used a transformation to concentrate data around UPOs making it easy to identify them as peaks in a histogram of the data. A sample of 256 IBIs was passively recorded and then transformed to scan for fixed points. The program re-analyzed the last 256 IBIs after every ten IBIs until it found a peak in the histogram of 90% or greater significance. In the interest of time, only ten Gaussian-shuffled surrogates of the 256 IBIs [14], [27], were used to calculate the statistical significance of these peaks; more surrogates might have increased our specificity but would have excessively increased the execution time (each surrogate added about 2 s). Because only ten surrogates were used, an additional criterion was used—the peak also had to be at the location of the maximum difference between the data and surrogate distributions.

### D. Control Procedures

1) *Control Algorithms*: All saddle fixed points (the type detected in previous studies of excitable systems [9], [14], [21], [23], [28], [29]) have an associated set of stable and unstable manifolds which can be approximated as lines within a small distance of the fixed point. The slopes of these manifolds were determined from the Jacobian matrix of the fixed point. Points along the stable manifold are attracted to the fixed point, while points along the unstable manifold are repelled by the fixed point. When the system state point wandered far enough away from the fixed point, the control algorithm issued a stimulus to shift the state point onto the stable manifold. The state point then moved toward the fixed point along the stable manifold on its own without further stimulation.

All of the experiments used SMP as the basic algorithm. When the state point fell outside of the control radius, control was activated. The control algorithm sent a stimulus to the slice to trigger a burst at the exact time needed to shift the state point onto the stable manifold. The advantage of using SMP was that the calculation of the desired IBI did not require estimation of the next “natural” IBI; instead, it was obtained through simple algebra. That is, the desired IBI value was given by

$$x_{n+1} = \lambda_s(x_n - x^*) + x^*. \quad (1)$$

where  $x_n$  was the current IBI,  $x^*$  was the fixed point, and  $\lambda_s$  was the eigenvalue (slope) of the stable manifold. The displayed IBIs were marked as stimulated or unstimulated. This assisted our assessment of the quality of control attained.

2) *Effect of Control Radius on Control Efficacy*: The effect of the size of  $R_c$  on control efficacy was investigated. After a fixed point was found by the UPO transform (UPOT),  $R_c$  was initially set to a large value (200 ms) and decreased in steps down to 2 ms during each experiment. No adaptive control algo-

ritms were used. Control efficacy was assessed using the variance of the IBIs as well as the percentage of IBIs that were stimulated versus natural.

3) *Adaptive Control Techniques*: Accurate estimates of the fixed point location and stable manifold slope were the two key elements needed to achieve good control. A technique developed by Christini and Kaplan [24] was used in an attempt to dynamically refine the approximation of these parameters. This method fits data to linear approximations of the dynamics in the neighborhood of the fixed point to re-estimate the fixed point and stable manifold slope. It was based on the assumption that the data were in the neighborhood of a UPO. As long as this was true, the unperturbed system dynamics could be approximated by the linear equation  $x_{n+1} = ax_n + bx_{n-1} + c$ , where the current state point was  $(x_{n-1}, x_n)$ . Rewritten in terms of the fixed-point parameters, this equation became

$$x_{n+1} = (\lambda_s + \lambda_u)x_n - \lambda_s\lambda_u x_{n-1} + x^*(1 + \lambda_s\lambda_u - \lambda_s - \lambda_u) \quad (2)$$

where  $x^*$  was the fixed point and  $\lambda_s$  and  $\lambda_u$  were the stable and unstable eigenvalues, respectively. When a control stimulus was applied, the system dynamics were described by

$$x_{n+1} = \hat{\lambda}_s(x_n - \hat{x}^*) + \hat{x}^* \quad (3)$$

where  $\hat{\lambda}_s$  signifies that  $\lambda_s$  and  $x^*$  were estimates, not the actual values. That is, when control stimuli were applied, they circumvented the normal fixed-point dynamics. Therefore, the natural values of  $\lambda_s$  and  $x^*$  could not be estimated from stimulated bursts. However, when unstimulated bursts occurred, the system would behave according to (2). The parameters  $x^*$ ,  $\lambda_s$ , and  $\lambda_u$  could then be estimated by a least-squares fit of the data triplets  $(x_{n+1}, x_n, x_{n-1})$ . Only “natural triplets”—those where  $x_{n+1}$  was an unstimulated IBI—were used. This regression was performed after every new natural triplet (or, equivalently, every natural IBI). This provided a method to refine the estimate of the fixed point and stable and unstable eigenvalues in real-time, which would improve the control of the system. Singular value decomposition (SVD) was used to perform the least-squares fit, in order to prevent poor fits. If the ratio between the fit’s largest and smallest singular values were very large ( $> 10^6$ ), then the fit would be poor. In that case, the parameter estimates would not be adjusted.

### E. State-Point Forcing

To help ascertain exactly what were the obstacles to control, a novel control protocol was developed [30]. Previously, the control algorithm only applied a single stimulus that placed the state point on the stable manifold estimate and let the system drift in to the fixed point on its own. In contrast, the new approach kept stimulating until the state point was on (or very close to) the fixed point in two dimensions. (Due to limitations in stimulus-burst interval precision, the state point could not always be forced exactly onto the fixed point, so it merely had to be within a small radius,  $R_{FP}$ , of the fixed point.) The stable manifold slope estimate was set to zero to minimize the amount of stimuli needed. If the fixed-point estimate were accurate, then the state point should remain close to the fixed point on the next iterate. However, if the fixed-point estimate were not accurate

(or no fixed point existed at that time), then the state point could end up anywhere on the next iterate. We, therefore, hypothesized that if we first forced the state point onto the fixed point and then forced it onto some other arbitrary point in the system attractor, the subsequent iterates should in general stay closer to the fixed point than to the arbitrary point. If there were a significant difference between the two cases, it would imply that the fixed-point estimate was relatively accurate.

To quantify these differences, we used the change in the center of mass ( $\Delta X_{cm}$ ) of the cluster of points around the forced point and after an iterate. The center of mass was calculated by computing the 2-D mean of the cluster of points that were within the fixed-point radius, and then the 2-D mean of the next iterates (images) of these points. The difference of these two means was  $\Delta X_{cm}$ . If the system state were forced onto a true fixed point, then  $\Delta X_{cm}$  should be small, while if it were forced onto an arbitrary point (or an inaccurate fixed-point estimate), then  $\Delta X_{cm}$  should be relatively big. Statistical comparisons of  $\Delta X_{cm}$  were made using the paired t-test or Wilcoxon signed rank test when the data did not pass a normality test (all tests computed with SigmaStat, Jandel Scientific).

### III. RESULTS

Bursts were recorded from the CA3 cell body layer and stimuli were applied in the Schaffer collaterals [Fig. 1(a)]. An example of a burst is shown in Fig. 1(b). The system state information was encoded as IBIs as seen in Fig. 1(c). One interesting result that was seen without control is shown in Fig. 2. These data came from a slice that went through a control experiment and then was allowed to spontaneously burst in preparation for another round of control. In Fig. 2(a), a return map, the bursting data resemble a checkerboard which would suggest a periodic pattern. When the 256 spontaneous IBIs are plotted versus IBI number in Fig. 2(b), it is evident that this is not a periodic pattern, but more like a chaotic one. We do not have an explanation for this intriguing behavior, which occurred in only one experiment.

#### A. Control of the Hénon Map

The control algorithms were first tested on the Hénon system to ensure their functionality.

1) *Basic SMP Control:* The basic SMP algorithm was tested first. A geometric interpretation of SMP control is shown in Fig. 3. Here,  $x_n$  represents the current IBI,  $\mathbf{z}_n = (x_{n-1}, x_n)$  is the current state point, and  $\mathbf{z}^* = (x^*, x^*)$  is the fixed point. When  $\mathbf{z}_n$  fell outside of the control radius, the control algorithm stimulated a “burst” at the exact time needed to shift the state point onto the stable manifold at  $\mathbf{z}_{n+1}$  (instead of  $\hat{\mathbf{z}}_{n+1}$ ).

The Hénon attractor is shown in Fig. 4(a). SMP control was tested for the Hénon map with and without added Gaussian noise. For the noiseless Hénon system, control worked well, but often produced period-2 or higher orbits, even though the algorithm was trying to control it to a period-1 orbit. An example of control to a period-1 orbit is shown in Fig. 4(b1). The system was confined within a very narrow range. Fig. 4(b2)

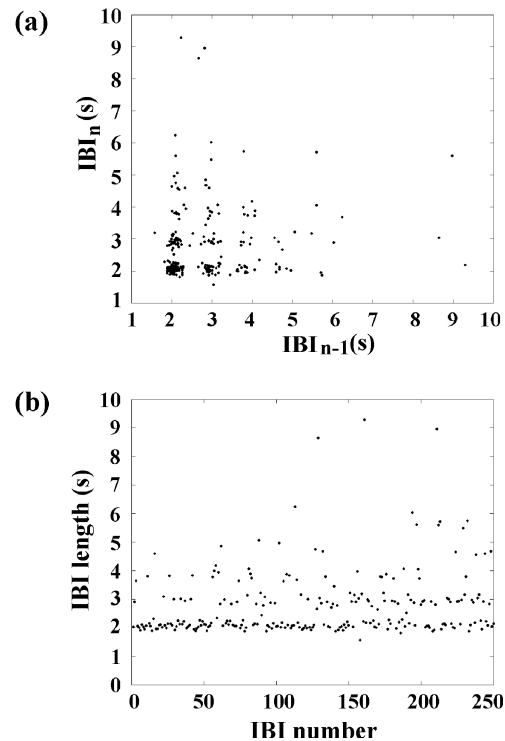


Fig. 2. Unusual spontaneous hippocampal bursting pattern. (a) When plotted as a return map, the IBIs form a checkerboard pattern, clustering around certain points. This appears to suggest a periodic pattern. However, when the IBIs are plotted versus IBI number (b), the behavior appears more chaotic than periodic. The system seems to jump chaotically between a few finite states (at approximately 2, 3, 4, and 5 s).

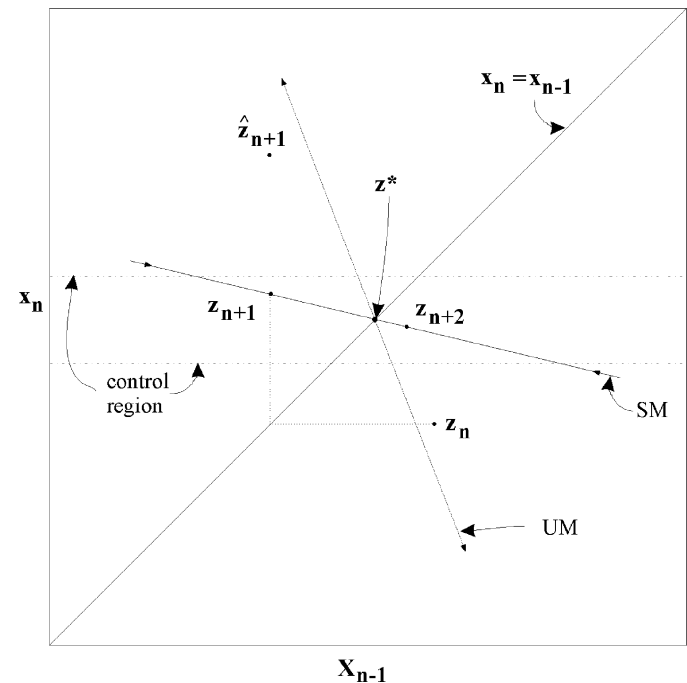


Fig. 3. Schematic of SMP control. Here,  $\mathbf{z}^*$  is the fixed point and  $\mathbf{z}_n$  is the current state point. Since  $\mathbf{z}_n$  is outside the control region, the goal is to get  $\mathbf{z}_n$  onto the stable manifold (SM). Since this is a return map, and the equation of SM is known,  $\mathbf{z}_{n+1}$  can be placed directly onto the stable manifold by “reflecting” (dotted line) off of the identity line and stimulating at this time. The unstable manifold does not need to be estimated for SMP.

shows a magnification of the controlled region. Iterates that were “stimulated” are shown as solid circles, and open circles

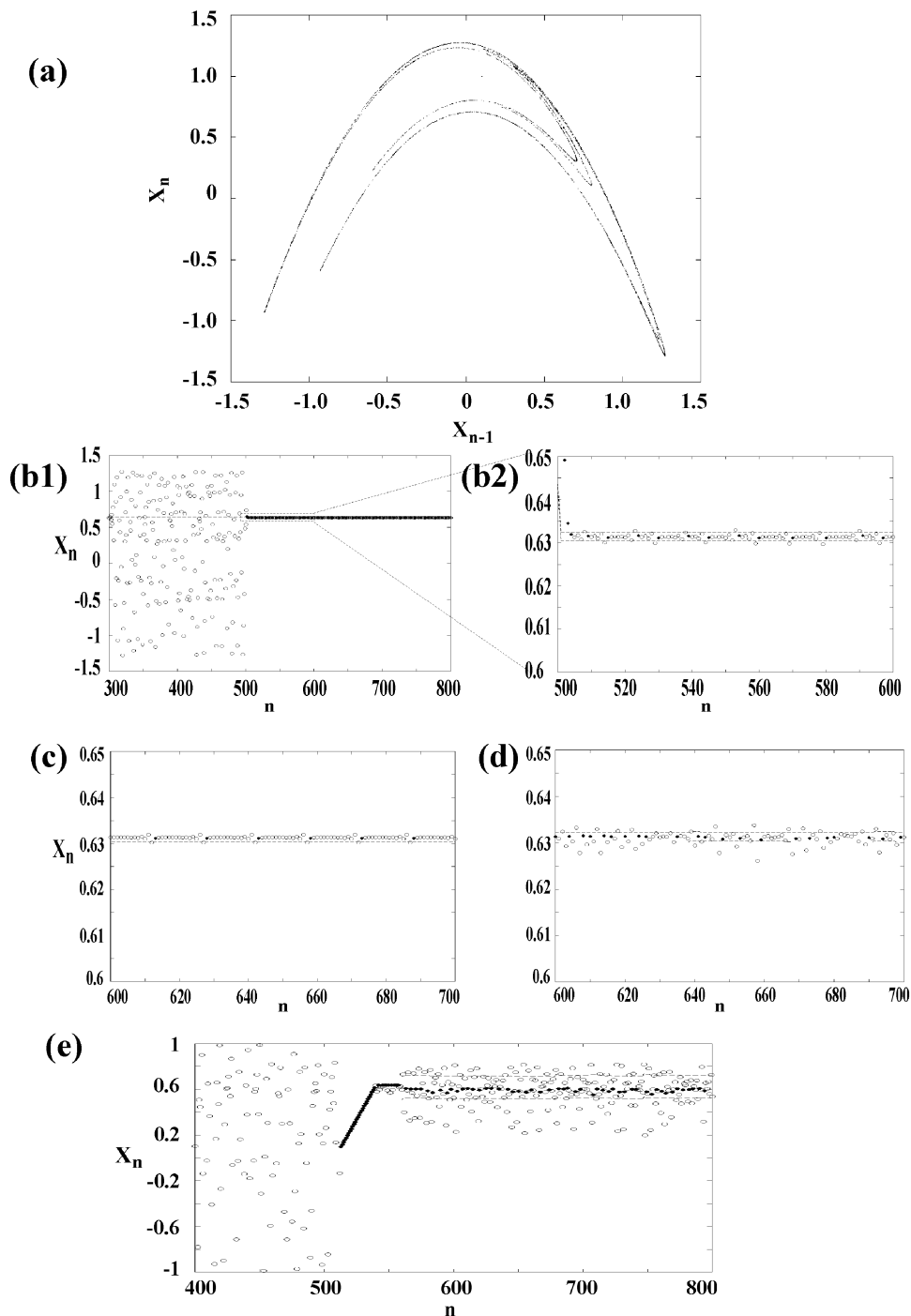


Fig. 4. Control of the Hénon system. (a) The Hénon attractor in delay coordinates, given by  $x_{n+1} = 1 - 1.4x_n^2 + 0.3x_{n-1}$ . (b) Control of the noiseless Hénon system. After 500 “unstimulated” iterates ( $\circ$ ), the fixed point was detected, and the control algorithm kept the system to within a very tight region. (B2) A magnified view of the box in (B1) shows that the system stayed within the control radius ( $R_c$ , dashed lines) for about nine iterates before needing another “stimulus” ( $\bullet$ ). (c) A magnified view of control using AT without noise and  $R_c = 0.001$  (dashed lines). Only 1 in 18 iterates were stimulated. (d) When low amplitude noise ( $\sigma = 0.0005$ ) was added, more stimuli were needed, but control was still very tight. (e) At higher noise levels ( $\sigma = 0.05$ ), control was not very tight and more stimuli were needed. However, the overall variance was still lower than before control started (0.026 versus 0.57). A scanning procedure (seen as a ramp of stimulated iterates of increasing length) was sometimes used to detect UPOs [32]. The presence of a period-doubling bifurcation denoted the location of the fixed point.

are “unstimulated” iterates. The dashed lines designate the control region around the fixed point. As expected, stimuli were not needed very frequently, approximately once in every nine iterates. When Gaussian noise was added, the quality of control deteriorated. As the standard deviation ( $\sigma$ ) of the noise increased

from 0.0005 to 0.05, the ability to control the system decreased: the variance of the data during control increased from  $7.7 \times 10^{-7}$  to 0.07. These values were calculated with the control radius ( $R_c$ ) set to  $2\sigma$ . The variance was reduced to 0.004 for  $\sigma = 0.05$  when  $R_c = 0.05$ ; however, more stimuli were needed. Also, the

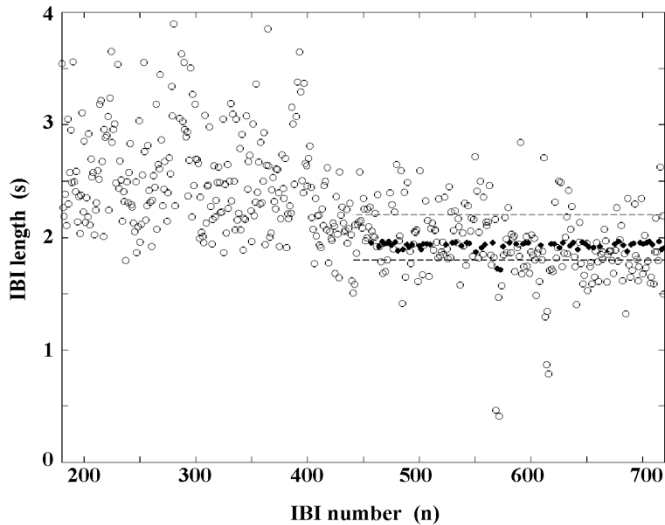


Fig. 5. An example of basic SMP control of bursting. After approximately 420 spontaneous bursts, a fixed point was found and the SMP control algorithm was applied with limited success. The variance during control was slightly lower than before control. The system did not stay within the control radius (0.2 s, dashed lines). IBIs were stimulated ( $\bullet$ ) versus natural ( $\circ$ ).

resulting data looked less and less like a periodic orbit as noise increased.

2) *Adaptive Re-Estimation by Triplet Regression*: Adaptive re-estimation, or tracking, immensely improved the quality of control. Adaptive tracking (AT) was also tested on the Hénon system with the addition of a small amount of drift to simulate nonstationarity. The drift was specified by the following modification to the Hénon equation:

$$x_{n+1} = 1 - (1.4 + \eta_n)x_n^2 + 0.3x_{n-1} \quad (4)$$

$$\eta_n = 0.999\eta_{n-1} + 0.00045\gamma_n \quad (5)$$

where  $\eta_n$  is an iterate of a correlated noise process and  $\gamma_n$  is a random number from a Gaussian distribution with unity standard deviation [24]. The noiseless Hénon system, seen in Fig. 4(c), was controlled using only one stimulus for every 18 iterates. As noise was added, control was still maintained, but more stimuli were needed. For example, Fig. 4(d) shows control for a noise level of  $\sigma = 0.0005$ , where about one in nine iterates were stimulated. For these experiments,  $R_c = 2\sigma$  (0.001 for  $\sigma = 0$ ), the number of natural triplets (NT) used in the SVD fit was ten, and the sample size for the UPOT was 250. When high-level noise was added ( $\sigma = 0.05$ ), the algorithm had a much more difficult time achieving control [Fig. 4(e)]. Many more stimuli were needed, and the system did not remain within the control region for very long. However, it remained very close to the control region, and was still kept to a much smaller region of phase space ( $\sigma = 0.026$ ) than the uncontrolled attractor ( $\sigma = 0.57$ ). The system controlled with added noise up to  $\sigma = 0.2$ . In addition, when drift was added to the system, the adaptive control algorithm continued to track well.

## B. Control of Epileptiform Bursting

1) *Basic SMP Control*: Tight control was not achieved for bursting data using basic SMP (Fig. 5). However, some reduc-

tion in variance was made over the uncontrolled bursting. There were several parameters that could affect the performance of this algorithm, including several parameters in the UPO detection algorithm. The number of nearest neighbors used to fit the Jacobian matrix for the UPOT was optimized to four, the same number for the Hénon map, since there was no notable effect of changing it. The control algorithm also had to account for the delay between the stimulus and the recorded burst due to finite conduction velocity in the tissue. This stimulus-burst delay was varied from 15–50 ms depending on the properties of each slice. It was kept constant during each experiment. Since the linear approximation of the stable manifold was only accurate within a small distance of the fixed point, we also tried applying control only when the previous state point was within a set radius ( $R_{UPO}$ ) of the fixed point.  $R_{UPO}$  was varied from 0.5–10 s, but there was no noticeable improvement in control quality. When  $R_{UPO}$  was small (0.5–1 s) and there were several long IBIs, sometimes it would take a long time before the system state would get close enough to the fixed point for control to resume.

2) *Effect of  $R_c$  and Synaptic Plasticity on Control Efficacy*: Previous work [31] suggested that stimulating the Schaffer collaterals at low frequencies ( $\sim 1$  Hz) could sometimes cause a form of synaptic plasticity called long-term depression (LTD), which could cause IBIs to lengthen over time. To assess whether some of the nonstationarity and impediments to control were due to this form of synaptic plasticity, the NMDA-receptor antagonist AP-5 was used. While LTD might occur using other receptors besides the NMDA type, AP-5 should block the majority of LTD via this pathway. Slices were bathed in high- $[K^+]_o$  ACSF for 20 min, and then in high- $[K^+]_o$  ACSF containing 50  $\mu$ M AP-5 (Tocris). The AP-5 solution was washed in for 5 min before starting the same control sequence used above with high- $[K^+]_o$ .  $R_c$  was again decreased in stepwise fashion.

The effect of  $R_c$  was assessed both with and without AP-5. Six experiments were done with high- $[K^+]_o$  only, and four were done using high- $[K^+]_o$  plus AP-5. Fig. 6 shows examples of experiments in which  $R_c$  was varied using high- $[K^+]_o$  only [Fig. 6(a)] or high- $[K^+]_o$  with AP-5 [Fig. 6(b)]. The inset to the right in Fig. 6(a) demonstrates the region where  $R_c$  was so small that nearly every IBI was stimulated. This phenomenon occurred because  $R_c$  was smaller (2 ms) than the precision of the stimulus-burst interval. That is, the interval from when the stimulus was applied to when the burst was detected fluctuated by a few milliseconds from burst to burst and, therefore, the estimate could be off by as much as 5 ms. Thus, the control algorithm kept stimulating but could not get the IBI within the control region. Since the algorithm was designed to continue stimulating until the last IBI was within the control region, the program was essentially effecting the equivalent of demand pacing, a protocol used in cardiac electrophysiology. This demand pacing-like phenomenon was consistently seen when  $R_c$  dipped down to 2 ms, and sometimes even at 10 ms.

In general, as  $R_c$  decreased, the variance of the IBIs (both natural and stimulated) decreased [Fig. 7(a)], and the percentage of IBIs that were stimulated increased [Fig. 7(b)]. This trend, while somewhat weak in the case of variance, was true for experiments both with ( $\bullet$ ) and without ( $\blacksquare$ ) AP-5. The mean of the

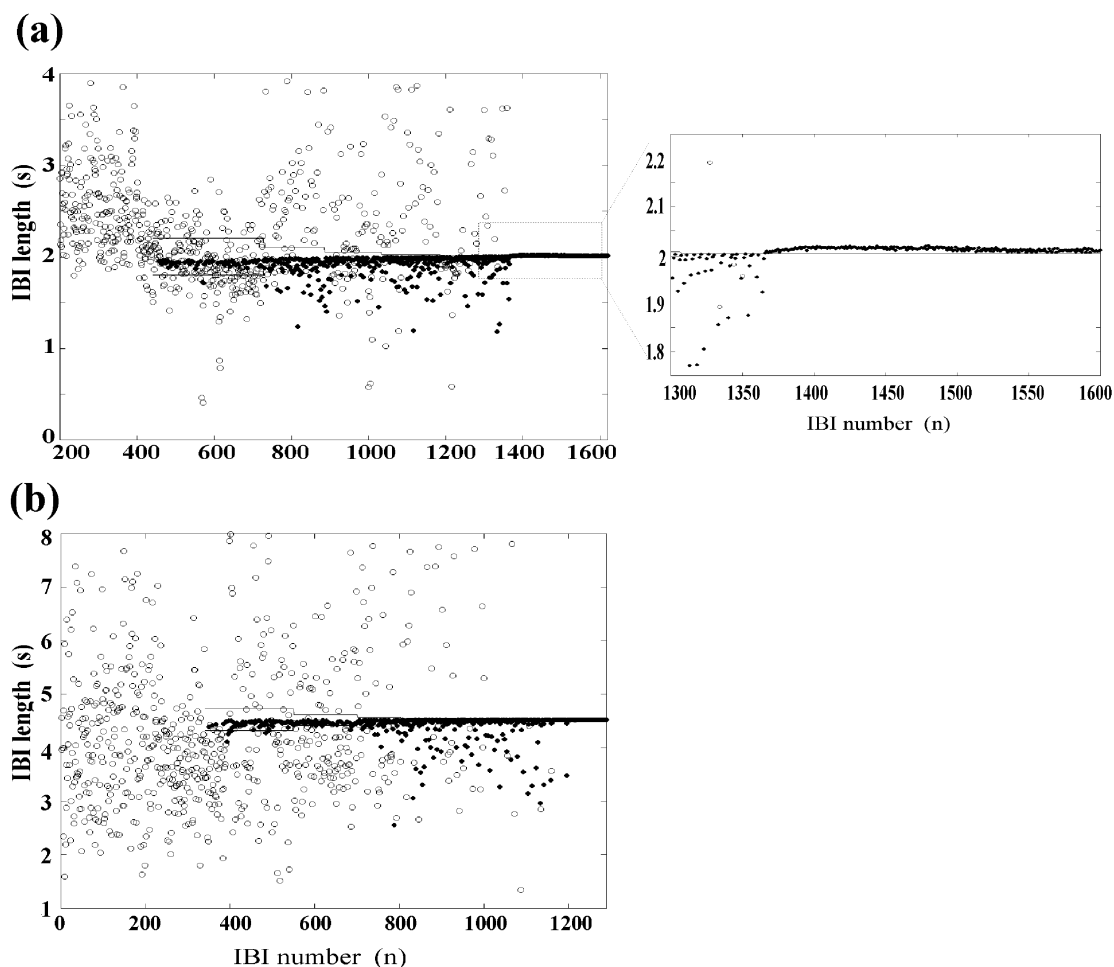


Fig. 6. Examples of experiments varying  $R_c$  and demand pacing. (a) A high- $[K^+]_o$  experiment using basic SMP control while varying control radius ( $R_c$ , solid lines). As  $R_c$  decreased, the variance also decreased, but the ratio of stimulated ( $\bullet$ ) to unstimulated ( $\circ$ ) IBIs increased. The magnification (right) of the boxed area shows the demand pacing phenomenon: all of the IBIs after IBI 1370 are stimulated, since the system never can get within the tiny  $R_c$ . (b) When  $R_c$  was varied in an experiment using AP-5, similar results were found. Thus, there did not appear to be any effects from LTD.

variances decreased from 1810 ms for  $R_c = 200$  ms to 390 ms for  $R_c = 2$  ms without AP-5, and from 450 ms to 76 ms with AP-5. Calculations using the median (instead of the mean) of the variances produced similar results. These experiments suggested that the optimal value of  $R_c$  was in the 50–100 ms range, depending on the variance of the system before control was started. Optimization consisted of balancing the percentage of stimuli used and the resulting tightness of control (variance) obtained. No apparent difference was seen between experiments with or without AP-5.

3) *Control Using AT via Triplet Regression:* Many trials ( $n = 43$ ) of control using AT were performed. AT noticeably improved control over basic SMP alone. Our refinements of the tracking algorithm and its parameters produced small but incremental improvements in control quality. An example of relatively good control using tracking is shown in Fig. 8(a). The control region (and, hence, the fixed point) tracks along smoothly with the drift of the system.

The least-squares fit itself had several notable caveats. The number of natural triplets used for the fit (NT) varied from 4–20. Too few triplets could cause poor fits and result in volatile fluctuations of the parameter values. Too many would not allow the algorithm to track the system quickly enough. Also, the

fit would sometimes not accurately represent the natural fixed-point dynamics. If most of the IBIs were stimulated, and then control were turned off, the state point would tend to shoot out from the fixed point along the unstable manifold. In this case, the stable manifold could not be estimated accurately since the state point would not approach the fixed point at all. If the majority of the NT triplets behaved this way, the fit would be very poor.

The number of triplets (NT) used in the fit was set to ten for all of the later experiments. Even when large values of NT (e.g., 10) were used, the fixed-point estimates often fluctuated. Therefore, the distance by which the fixed-point estimate could change from the current estimate in any one fit was limited. This parameter, called the fixed-point adjustment maximum (FAM), was optimized and normally set in the range of 0.5–1 s, in proportion to the initial variance of the system. This adjustment helped a good deal in reducing variability. However, if FAM was set too small, the algorithm would not adapt well. Another modification allowed the algorithm to only include natural triplets in the fit if the natural IBIs were within a certain radius ( $R_{NT}$ ) of the current fixed-point location. Since the linear least squares fit was only valid within a small radius of the fixed-point location, any natural IBIs that were far away from the current fixed

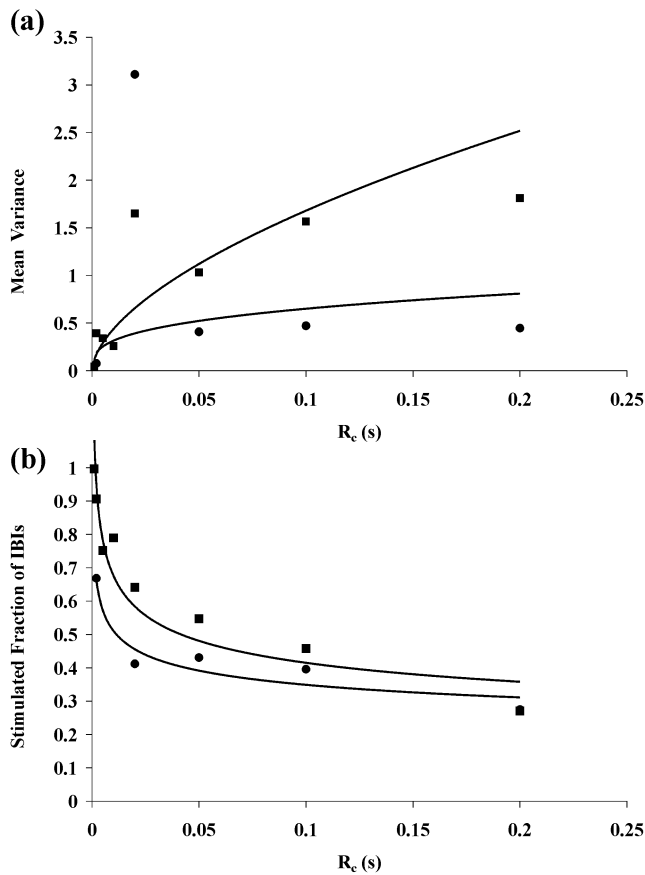


Fig. 7. Summary of effects of  $R_c$  and synaptic plasticity on control of bursting. (a) As  $R_c$  decreased, the mean variance of the IBIs also tended to decrease. This was true for experiments with (●) and without (■) AP-5. (b) As  $R_c$  decreased, the fraction of IBIs that were stimulated increased for both types of experiments.

point (i.e., outliers) but were still included in previous fits would cause a poor fit. Improving the fit also reduced fluctuations in the fixed-point estimates. The optimal range for  $R_{NT}$  was about 0.4–1 s, depending on the variance of all the data.

At times, the control algorithm appeared to produce a period-1, -2 or -3 orbit that would last for some 6–12 IBIs during the course of an experiment. Two such period-2 orbits are seen in Fig. 8(b). The first one alternated between 2.3 and 2.7 s, for about 10–12 IBIs, starting near IBI #375. The second one occurred near IBI #920 in the same experiment but only remained for about six IBIs. These “close approaches” to period-2 orbits were seen in different experiments, but recurrence to the same period-2 orbit later in the experiment was not usually seen probably due to nonstationarity. Similar encounters were seen with period-1 orbits.

4) *Feasibility of Control and Fixed-Point Detection by State-Point Forcing:* The state-point forcing protocol was first tested on the Hénon map to make sure it could distinguish valid fixed points. There was a clear difference between forcing to the fixed point and forcing to an arbitrary point [Fig. 9(a)], even with added noise (which inhibited the accuracy of fixed-point detection). State-point forcing was then applied to bursting in 22 experiments (on 16 slices from 11 rats) to a total of 102 fixed points. Slices were bathed in high- $[K^+]_o$  ACSF and fixed points were detected as described above. When a significant fixed point

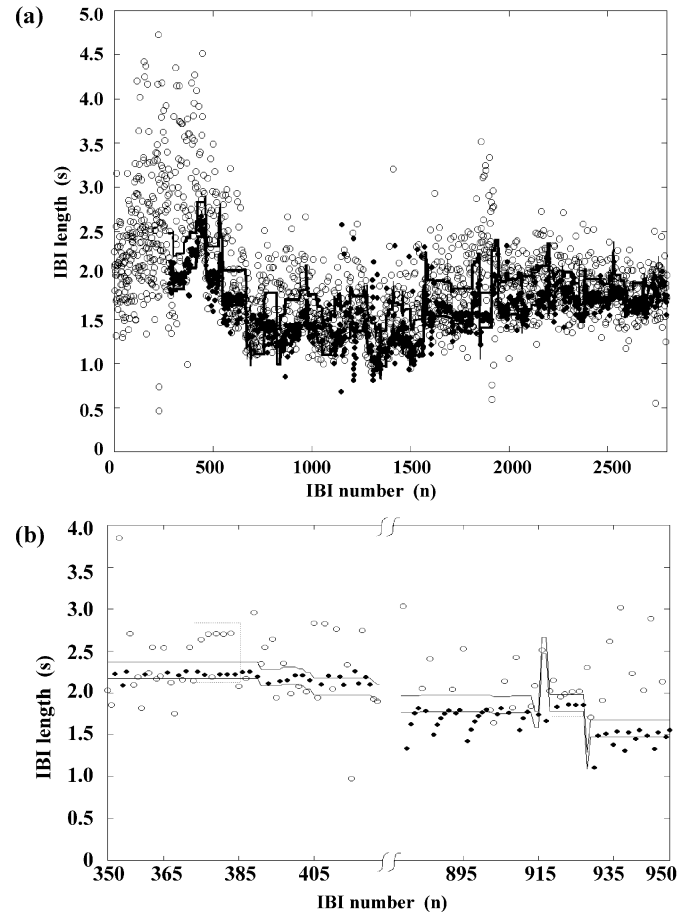


Fig. 8. Control of bursting using AT. (a) An example of a tracking experiment. The fixed-point estimate and control region (solid lines) tracks along well with the system. Variance is relatively low, but a large amount of stimulated IBIs (●) are still needed. (b) Two brief encounters with possible period-2 orbits in one experiment, shown in the dashed boxes near IBIs 375 and 920.

was found, the state point was forced onto the fixed point for 30–40 IBIs, and then onto an arbitrary point for 30–40 IBIs. The fixed-point radius,  $R_{FP}$ , was set to 40 ms. The forcing point alternated between the fixed point and the arbitrary point from 2–5 times, until the fixed point seemed to be drifting due to nonstationarity. At this point, if the slice was still bursting quickly enough, state-point forcing was turned off and AT was initiated to relocate the fixed point. If a suitable fixed-point estimate was found (i.e., tracking seemed to be working and had stabilized at one location after a while), then tracking was turned off, state-point forcing was turned back on, and  $\lambda_s$  was set to zero. Again the forcing point alternated between the new fixed point and an arbitrary point 2–5 times. An example of a state-point forcing experiment is shown in Fig. 9(b).

The value of  $\Delta X_{cm}$  was computed for each fixed point and its corresponding arbitrary forcing point. The fixed-point trials were evenly split (51 each) between those detected with the UPOT and those found with the AT algorithm. Statistical comparisons of  $\Delta X_{cm}$  were made with the paired t-test or the Wilcoxon signed rank test. The data were first compared for both UPO types combined, and  $\Delta X_{cm}$  was significantly smaller when forcing to the fixed points than to the arbitrary points (median values 0.258 s versus 0.404 s,  $P < 0.004$ , signed

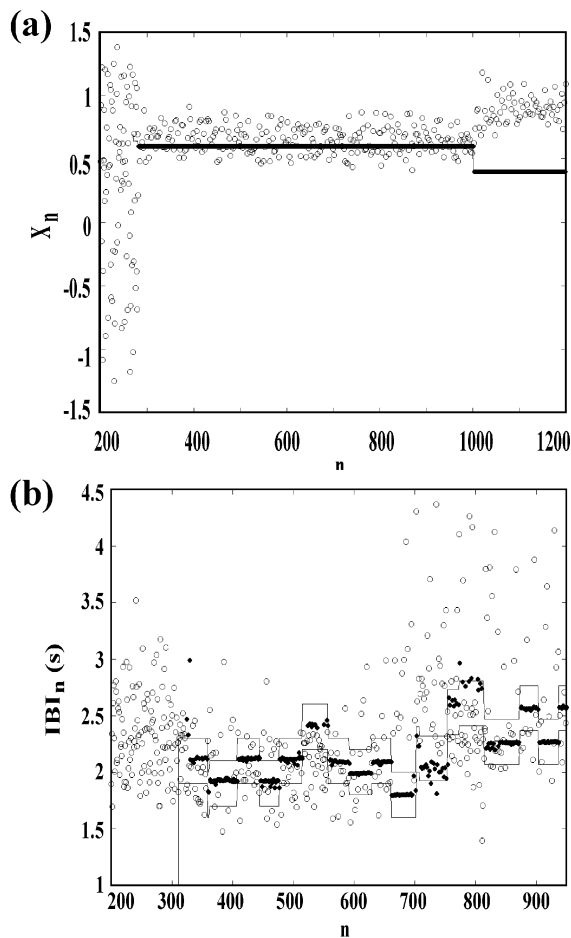


Fig. 9. State-point forcing for Hénon and bursting experiments. State-point forcing was first tested on the Hénon map with added noise ( $\sigma = 0.1$ ). (a) Once the fixed point was found, the system state was forced to it until  $n = 1000$ ; then the system state was forced to a point 0.2 away from the fixed point. As expected, when the system was forced to the fixed-point estimate (at 0.6, actual fixed point: 0.6314) by stimulating ( $\bullet$ ), the next (unstimulated,  $\circ$ ) iterates stayed very close to the fixed point. But when the system state was forced to an arbitrary point (at 0.4), the next iterates were up near 0.9. (b) An example of forcing in a bursting experiment. Forcing alternated between the fixed point and arbitrary points four times (counted as four fixed-point trials in analysis). Then tracking was turned on (at  $n \sim 700$ ) until a new fixed point was found at  $n = 820$ . Tracking was then turned off and forcing turned back on. Natural IBIs stayed closer to fixed points than to arbitrary points.

rank test). The UPOT fixed points alone did not show a significant difference in  $\Delta X_{cm}$ , but the AT fixed points did have significantly smaller  $\Delta X_{cm}$  when forcing to the fixed versus arbitrary point.

The data were split up in several ways for further analysis (Table I). The arbitrary forcing point was set both greater than (positive) and less than (negative) the fixed point in several trials. When it was positive, the natural IBIs were sometimes shorter than the forcing point, so not enough data points could be obtained for the analysis. The arbitrary point was 0.1–0.4 s away (both positive and negative) from the fixed point, proportional to the size of the system attractor. Usually the shift was 5%–15% of the attractor width. The differences in  $\Delta X_{cm}$  were significant for negative shifts, but were not significant for positive shifts. When AT and UPOT data were analyzed separately, negative shifts were significantly different for both

TABLE I  
SUMMARY OF FORCING PROTOCOL  
RESULTS USING  $\Delta X_{cm}$  FOR DIFFERENT CATEGORIES OF FIXED POINTS.  
P-VALUES WERE DETERMINED USING EITHER PAIRED T-TEST (PTT) OR  
(WHEN NORMALITY TEST WAS FAILED) THE WILCOXON SIGNED RANK TEST  
(WSRT). UPOT, FIXED POINTS FOUND WITH THE UPO TRANSFORM; AT,  
FIXED POINTS FOUND WITH ADAPTIVE TRACKING

Category	# of points	P-value	Median $\Delta X_{cm}$ for fixed point	Median $\Delta X_{cm}$ for arbitrary point	Type of test
All fixed points	102	0.0038	0.26	0.40	WSRT
UPOT	51	0.074	0.46	0.41	WSRT
AT	51	0.015	0.22	0.38	WSRT
All points shifted down	53	<0.0001	0.18	0.41	WSRT
All points shifted up	49	0.80	0.49	0.39	WSRT
UPOT shifted down	23	0.043	0.24	0.34	WSRT
AT shifted down	30	<0.0001	0.15	0.45	WSRT
UPOT shifted up	28	0.76	0.53	0.40	WSRT
AT shifted up	21	0.57	0.81	0.74	PTT

AT and UPOT, while positive shifts were not significantly different for either. The AT fixed points tended to have smaller P values than UPOT fixed points.

#### IV. DISCUSSION

##### A. Insights From the Hénon Simulations

Control of the Hénon map was achieved with the basic SMP algorithm. AT using triplet re-estimation was successful in controlling the Hénon map with noise levels up to  $\sigma = 0.2$  (15% of the attractor size; more noise made the system state approach infinity) and with added random drift. However, while the variance was low relative to the system as a whole, many more stimuli were used at high noise levels. This implied that in a strongly deterministic system, if enough stochastic noise were present it would be difficult to achieve control with few stimuli. Yet control to a relatively small region would still be possible, and the number of stimuli needed would still be fewer than periodic pacing would use.

Another important implication from the Hénon simulation was that the fixed-point location was not found precisely very often for the Hénon map, even without noise. The fixed-point estimate often varied by up to 0.1 (3%) from the correct estimate of 0.631. This may seem small, but the result of control, even with AT, was usually a period-2 orbit.

##### B. Control of Bursting With SMP and AT

Control of bursting using the basic SMP algorithm showed limited success. The variance during control did decrease but not enough to be considered tight control.

1) *Effect of Control Radius Size and Synaptic Plasticity on Control Efficacy:* The size of the control radius  $R_c$  was an important determinant of the quality of control obtained. Experiments that varied  $R_c$  were often difficult to interpret because of several confounding factors. Nonstationarity was a problem because the fixed-point locations had to be constant over the

course of the experiment which could last up to 2500 IBIs. Thus, there was plenty of time for the fixed points to drift or disappear. Also, when stimulating the slice more frequently (as tended to happen as  $R_c$  decreased), the natural IBIs often lengthened, either because the slice was “fatigued” or because of synaptic plasticity (i.e., LTD). Extremely long IBIs (15–40 s) sometimes occurred, and these “outliers” skewed the results by disproportionately increasing the variance. Previous studies had suggested that low frequency stimulation could cause LTD during bursting with lengthened IBIs as time passed [31]. Some experiments did seem to produce this gradual lengthening effect as the experiment progressed; however, the same effect was seen in some of the experiments using the NMDA-receptor antagonist AP-5. The majority of experiments varying  $R_c$  did not show lengthening of the IBIs. Moreover, in one experiment, control was shut off near the end of the experiment and the IBI profile was the same as it was before control had started—i.e., the length did not increase due to stimulation.

With these caveats taken into account, the results of our experiments nonetheless indicated that as  $R_c$  decreased, variance decreased but the proportion of IBIs that were stimulated increased. This conclusion was true for both the standard high- $[K^+]_o$  experiments and for experiments using AP-5. This similarity of results suggested that synaptic plasticity does not significantly influence the quality of control obtained. We found that the control radius that optimally balanced variance versus number of stimuli was usually 50–100 ms depending on the initial variance of the bursting.

At extremely small control radii, the system performed almost identically to demand pacing. Interestingly, the results looked very similar to those obtained by Schiff *et al.* [9], as well as Christini and Collins [13], especially if the IBIs were not designated as stimulated or natural. Since their work did not make this distinction, it could be possible that their control algorithm was constantly stimulating due to a very small control radius. This could explain why the control of bursting results in the present study do not seem as striking as those reported earlier [9].

2) *AT*: To overcome the obstacle of nonstationarity, we used the method of AT to refine our estimates of the fixed point and stable manifold slope after every natural IBI. While the results using this technique were not dramatic, they were a definite improvement over basic SMP control. At first, the tracking algorithm produced some fluctuations in the fixed-point estimates which inhibited control. After adding regulating parameters such as the FAM and  $R_{NT}$ , the fixed-point estimate tracked with the system smoothly over time. Even with these modifications, triplet regression would still occasionally make “illogical” adjustments to the fixed-point location. For example, when all the natural IBIs were greater than the fixed point, the new fixed-point estimate would still sometimes be set smaller than the current estimate. We, therefore, required that the new estimate move in the same direction as most of the natural IBIs are located relative to the current fixed point. This modification helped stabilize control. The variance during tracking control was much less than that during basic SMP but not as low, relative to the initial variance before control, as for the Hénon map with the highest level of noise ( $\sigma = 0.2$ ).

On several occasions in tracking experiments, the system briefly remained in a period-1, -2, or -3 orbit for a short time. These close encounters provided tantalizing hints that control was indeed possible, at least for short periods of time. The fact that higher-period orbits were attained more often than period-1 orbits suggested that the fixed-point estimate was close but not quite accurate enough.

### C. State-Point Forcing

We designed the state-point forcing protocol to ascertain whether control was at all feasible and to help identify the obstacles in detail. Specifically, we sought to verify that our fixed-point estimates were valid. Also, if the system state would not stay close to the fixed point for a few iterates even when placed directly onto the fixed point, then no control short of pacing would have much chance of working. The results of the forcing experiments suggested that the fixed-point estimates were indeed valid, since forcing onto the fixed points produced significantly less divergence in the subsequent iterate than did forcing onto the arbitrary points.

More detailed analysis revealed that forcing to fixed points found with AT produced significant results whereas those found with the UPOT did not. This suggested that perhaps the AT provided better estimates of the fixed point than did the UPOT algorithm. When the UPOT was applied offline to 22 sets of state-point forcing data, only 23% of the fixed points detected online (using ten surrogates) were found to be statistically significant offline (using 50 surrogates). This could be the reason that the forcing protocol did not produce significant results for UPO-transformed fixed points. Moreover, it is possible that much of the difficulty we had with control was due to inaccurate or false fixed-point estimates. Another notable result was that when the arbitrary forcing point was shorter than the fixed point, the difference in  $\Delta X_{cm}$  was strongly significant ( $P < 0.0001$ ), whereas when the arbitrary forcing point was longer than the fixed point, the difference in  $\Delta X_{cm}$  was not significant ( $P = 0.8$ ). This result could be explained in two ways. The first is artifactual: when the arbitrary point was shifted up, the neurons often burst naturally before stimuli could be applied and, thus, there were fewer points that could be used in the calculation of  $\Delta X_{cm}$ . Alternatively, when the arbitrary point was shifted down, the stimuli would be occurring more quickly, thus giving the slice less time to recover and, therefore, the next natural bursts could have been longer simply because the slice was “fatigued” or refractory. We tried to avert this second possibility by shifting the arbitrary point by different amounts, in a range from 0.1 s to 0.4 s.

### D. Obstacles to Control and Necessary Assumptions

The implications of these results for the feasibility of control were not as clear. The next IBIs (after a stimulated burst) stayed relatively close to the fixed points, although not as close as would be required to obtain tight control. This may have been due to the high levels of stochastic dynamical noise that were also present in the system. A high level of noise certainly would have hindered attempts to control the system—especially if it were on the order of the control radius—since the system state would often bounce out of the control region as soon as

it was placed within it. It would have also complicated the calculation of the fixed point and stable manifold. Unfortunately, there was no way of empirically determining the level of noise in the system, so we could not determine whether noise was the biggest impediment to control.

Estimation of the stable manifold was itself a very difficult task. Even with a low-noise system, the method of fitting local neighbors of the fixed point using a linear least-squares algorithm was a simplification. It is doubtful that the manifolds were linear, so any linear approximation would only be accurate within a very small radius of the fixed point. It is possible (due to small sample size) that the four neighbors used for the Jacobian were often outside of this linear region. With the addition of high-level noise, fitting the stable manifold could become problematic because there are too few natural triplets that approach the fixed point.

Several necessary assumptions were made that may have had an effect on the ability to control the system. The use of IBIs as our state variable was somewhat arbitrary. It was mainly a matter of convenience and convention [9], [21]. The use of IBIs may have contributed to the effect of noise since they vary on a long time scale and, thus, many factors can change in between each measurement. Perhaps using a variable such as the raw extracellular voltage could have improved the results. However, it would have been extremely difficult to precisely control extracellular voltage levels using a point-source electrode. Also, the embedding dimension equal to two that was used could have been too small. However, we used it because it greatly simplified the calculations and because it was the same dimension used as previously reported by Schiff *et al.* [9]. All of these assumptions were necessary to make but also could have compromised control efficacy if they were inaccurate.

Finally, the phenomenon of nonstationarity was a large obstacle to control. Large drifting was evident by inspection (e.g., monitoring the mean IBI rate). There were many potential sources for drift. Fluctuations in flow rate could easily have altered the system behavior by affecting the concentrations of key nutrients and temperature. Fluctuations of temperature due to bath levels and ambient air temperature may also have been a problem. There also could have been intrinsic nonstationarity in the bursting itself. Synaptic plasticity did not appear to have a significant effect, but it is possible that the slice became “fatigued” or refractory. We attempted to control for fatigue by ensuring that burst amplitudes remained constant throughout the experiment, since burst amplitude is an indicator of neurotransmitter supply [31].

## V. CONCLUSION

Chaos control techniques showed modest success at controlling spontaneous epileptiform bursting. AT noticeably improved control over nonadaptive methods and seemed to counter nonstationarity, but intrinsic randomness may have prevented us from obtaining tight control. The process of slicing the hippocampus itself severs many regulatory connections, both extrinsic and intrinsic. It is possible that the intact brain could be less noisy or more stationary than the *in vitro* hippocampal slice and, hence, easier to control.

In this investigation, we have attempted to manipulate the system from a chaotic trajectory to a low-period orbit. It is still not known whether controlling interictal bursts or spikes (or anticontrolling, i.e., making them more disordered) could prevent a seizure. Nor is it known how tightly the spikes would have to be controlled to be successful. However, if we could maneuver the system from a chaotic to a periodic state, then it is likely that we could also convert it from a periodic to a chaotic one. Once we have established the ability to manipulate the system, we could then determine whether a chaotic or periodic rhythm would be desirable to stop or prevent seizure activity. Thus, continued exploration should help reveal whether chaos control is a practical solution for preventing epileptic seizures.

## ACKNOWLEDGMENT

The authors would like to thank D. Christini and D. Kaplan for their helpful and insightful conversations and suggestions.

## REFERENCES

- [1] B. J. Gluckman, H. Nguyen, S. L. Weinstein, and S. J. Schiff, “Adaptive electric field control of epileptic seizures,” *J. Neurosci.*, vol. 21, pp. 590–600, Jan. 2001.
- [2] P. Boon, K. Vonck, M. D’have, S. O’Connor, T. Vandekerckhove, and J. De Reuck, “Cost-benefit of vagus nerve stimulation for refractory epilepsy,” *Acta Neurologica Belgica*, vol. 99, pp. 275–280, Dec. 1999.
- [3] G. L. Morris III and W. M. Mueller, “Long-term treatment with vagus nerve stimulation in patients with refractory epilepsy. The Vagus Nerve Stimulation Study Group E01-E05,” *Neurology*, vol. 53, pp. 1731–1735, Nov. 1999.
- [4] J. F. Annegers, S. P. Coan, W. A. Hauser, and J. Leestma, “Epilepsy, vagal nerve stimulation by the NCP system, all-cause mortality, and sudden, unexpected, unexplained death,” *Epilepsia*, vol. 41, pp. 549–553, May 2000.
- [5] J. I. Sirven, M. Sperling, D. Naritoku, S. Schachter, D. Labar, M. Holmes, A. Wilensky, J. Cibula, D. M. Labiner, D. Bergen, R. Ristanovic, J. Harvey, R. Dasheiff, G. L. Morris, C. A. O’Donovan, L. Ojemann, D. Scales, M. Nadkarni, B. Richards, and J. D. Sanchez, “Vagus nerve stimulation therapy for epilepsy in older adults,” *Neurology*, vol. 54, pp. 1179–1182, Mar. 2000.
- [6] F. Velasco, M. Velasco, A. L. Velasco, F. Jimenez, I. Marquez, and M. Rise, “Electrical stimulation of the centromedian thalamic nucleus in control of seizures: long-term studies,” *Epilepsia*, vol. 36, pp. 63–71, Jan. 1995.
- [7] R. S. Fisher, G. L. Krauss, E. Ramsay, K. Laxer, and J. Gates, “Assessment of vagus nerve stimulation for epilepsy: report of the therapeutics and technology assessment subcommittee of the American Academy of Neurology,” *Neurology*, vol. 49, pp. 293–297, July 1997.
- [8] R. B. Banzett, A. Guz, D. Paydarfar, S. A. Shea, S. C. Schachter, and R. W. Lansing, “Cardiorespiratory variables and sensation during stimulation of the left vagus in patients with epilepsy,” *Epilepsy Res.*, vol. 35, pp. 1–11, May 1999.
- [9] S. J. Schiff, K. Jerger, D. H. Duong, T. Chang, M. L. Spano, and W. L. Ditto, “Controlling chaos in the brain,” *Nature*, vol. 370, pp. 615–620, Aug. 1994.
- [10] J. Gotman and M. G. Marciani, “Electroencephalographic spiking activity, drug levels, and seizure occurrence in epileptic patients,” *Ann. Neurol.*, vol. 17, pp. 597–603, 1985.
- [11] S. F. Traynelis and R. Dingledine, “Potassium-induced spontaneous electrographic seizures in the rat hippocampal slice,” *J. Neurophys.*, vol. 59, pp. 259–276, Jan. 1988.
- [12] M. Barbarosie and M. Avoli, “CA3-Driven hippocampal-entorhinal loop controls rather than sustains *in vitro* limbic seizures,” *J. Neurosci.*, vol. 17, pp. 9308–9314, Dec. 1997.
- [13] D. J. Christini and J. J. Collins, “Controlling nonchaotic neuronal noise using chaos control techniques,” *Phys. Rev. Lett.*, vol. 75, pp. 2782–2785, Oct. 1995.
- [14] M. W. Slutzky, P. Cvitanovic, and D. J. Mogul, “Deterministic chaos and noise in three *in vitro* hippocampal models of epilepsy,” *Ann. BME*, vol. 29, pp. 607–618, July 2001.

- [15] L. D. Iasemidis and J. C. Sackellares, "Chaos theory and epilepsy," *Neuroscientist*, vol. 2, pp. 118–126, 1996.
- [16] J. C. Sackellares, L. D. Iasemidis, R. L. Gilmore, and S. N. Roper, When chaos fails, in *Chaos in the Brain?*, K. Lehnertz and C. E. Elger, Eds., World Scientific, Singapore, pp. 1–22, 2000.
- [17] D. Auerbach, P. Cvitanovic, J.-P. Eckmann, G. Gunaratne, and I. Procaccia, "Exploring chaotic motion through periodic orbits," *Phys. Rev. Lett.*, vol. 58, pp. 2387–2389, June 1987.
- [18] E. Ott, C. Grebogi, and J. A. Yorke, "Controlling chaos," *Phys. Rev. Lett.*, vol. 64, pp. 1196–1199, Mar. 1990.
- [19] E. R. Hunt, "Stabilizing high-period orbits in a chaotic system: the diode resonator," *Phys. Rev. Lett.*, vol. 67, pp. 1953–1955, Oct. 1991.
- [20] K. Pyragas, "Continuous control of chaos by self-controlling feedback," *Phys. Lett. A*, vol. 170, pp. 421–428, 1992.
- [21] A. Garfinkel, M. L. Spano, W. L. Ditto, and J. N. Weiss, "Controlling cardiac chaos," *Science*, vol. 257, pp. 1230–1234, Aug. 1992.
- [22] M. Z. Ding, W. M. Yang, V. In, W. L. Ditto, M. L. Spano, and B. Gluckman, "Controlling chaos in high dimensions: theory and experiment," *Phys. Rev. E*, vol. 53, pp. 4334–4344, May 1996.
- [23] D. J. Christini and J. J. Collins, "Control of chaos in excitable physiological systems: a geometric analysis," *Chaos*, vol. 7, pp. 544–549, Dec. 1997.
- [24] D. J. Christini and D. T. Kaplan, "Adaptive estimation and control method for unstable periodic dynamics in spike trains," *Phys. Rev. E*, vol. 61, pp. 5149–5153, May 2000.
- [25] P. Horowitz and W. Hill, *The Art of Electronics*, 2nd ed. New York: Cambridge Univ. Press, 1989.
- [26] P. So, E. Ott, T. Sauer, B. J. Gluckman, C. Grebogi, and S. J. Schiff, "Extracting unstable periodic orbits from chaotic time series data," *Phys. Rev. E*, vol. 55, pp. 5398–5417, May 1997.
- [27] J. Theiler, S. Eubank, A. Longtin, B. Galdrikian, and J. D. Farmer, "Testing for nonlinearity in time series: the method of surrogate data," *Physica D*, vol. 58, pp. 77–94, 1992.
- [28] X. Pei and F. Moss, "Characterization of low-dimensional dynamics in the crayfish caudal photoreceptor," *Nature*, vol. 379, pp. 618–621, Feb. 1996.
- [29] P. So, J. Francis, T. I. Netoff, B. Gluckman, and S. J. Schiff, "Periodic orbits: a new language for neuronal dynamics," *Biophys. J.*, vol. 74, pp. 2776–2785, 1998.
- [30] M. W. Slutzky, P. Cvitanovic, and D. J. Mogul, "Identification of determinism in noisy neuronal systems," *J. Neurosci. Methods*, 2002.
- [31] J. S. Bains, J. M. Longacher, and K. J. Staley, "Reciprocal interactions between CA3 network activity and strength of recurrent collateral synapses," *Nat. Neurosci.*, vol. 2, pp. 720–726, Aug. 1999.
- [32] D. T. Kaplan, "Exceptional events as evidence for determinism," *Physica D*, vol. 73, pp. 38–48, May 1994.



**Marc W. Slutzky** (S'97–M'02) received the B.S. degree in electrical engineering with highest honors from the University of Illinois at Urbana-Champaign in 1994. He received the Ph.D. degree in biomedical engineering from Northwestern University, Evanston, IL, in 2000 for his research on the application of nonlinear dynamical systems theory to characterization and control of epileptiform activity. In 2002, he received the M.D. degree from Northwestern University Medical School.

He is currently a Neurology Resident at the McGaw Medical Center of Northwestern University, Chicago. His research interests include nonlinear dynamics, neural prosthetics, neuroengineering, and neurophysiology.



**Predrag Cvitanovic** holds the Robinson Chair in Nonlinear Science and is the Director of the Center for Nonlinear Science at the Georgia Institute of Technology, Atlanta. He has been Professor with the Department of Physics and Astronomy, Northwestern University, Evanston, IL, and Director of the Center for Chaos and Turbulence Studies and Carlsberg Foundation Research Professor at the Niels Bohr Institute in Copenhagen, Denmark. His research interests include nonlinear dynamics, chaos, quantum chaos, the topology of hyperbolic flows, statistical mechanics, and turbulence. His best known work is the theory of cycle expansions—that is, expansions based on using periodic orbit theory—to approximate chaotic dynamics in a controlled perturbative way.

Prof. Cvitanovic and collaborators are currently completing an advanced graduate classical and quantum chaos textbook, available in electronic form at [www.nbi.dk/ChaosBook/](http://www.nbi.dk/ChaosBook/).



**David J. Mogul** (S'77–M'79) received the B.S. degree in electrical engineering from Cornell University, Ithaca, NY, in 1979. He received the M.S. and Ph.D. degrees in electrical engineering/computer science from Northwestern University, Evanston, IL, in 1984 and 1988, respectively.

After completing a research fellowship at the University of Chicago, Chicago, in 1992, he joined the faculty of Biomedical Engineering at Northwestern University, Evanston, IL, as an Assistant Professor.

He has served as a key consultant to a number of major pharmaceutical and medical device corporations. He is currently an Associate Professor of Biomedical Engineering at the Illinois Institute of Technology, Chicago. His research interests include brain electrophysiology, nonlinear control of epilepsy, neuroengineering, and ionic and receptor mechanisms underlying memory. He is a reviewer for both neuroscience and engineering publications.